Araştırma Makalesi / Research Article

Numerical Analysis of Temperature Distribution in Tandem Welding Process

Osman UNAL[1*], Nuri AKKAS[2]

Abstract

In this study, the numerical solutions for the steady-state heat conduction problem with uniform heat source, the steady-state heat conduction problem with convective heat transfer and the transient heat conduction problem have been developed using finite difference method. These numerical solutions have been validated with analytical solutions. After observing the good agreements between numerical solutions and analytical solutions, these three different problems combined to simulate the tandem welding process. The first objective of this study is to present a numerical simulator for the transient heat conduction problem that includes non-uniform moving heat sources and convective heat transfer term. This numerical simulator contains explicit and implicit time discretization methods. In this simulator, it is possible to change the grid sizes, time step sizes, total simulation time, distance between electrodes, magnitude of the sources' power, speed of the sources, etc. Secondly, the temperature distribution of single and twin wire welding processes have been compared using proposed numerical simulator to investigate the premature solidification of liquid metal in low-temperature zone of molten pool. Thirdly, experimental study was carried out using Fluke Thermal Imager to validate numerical results. It was obtained that the maximum temperature of numerical result is very close to the maximum temperature of experimental result with 0.248 % error. Finally, the all Matlab codes related to developed numerical simulator have been added to Appendix to facilitate other researchers' work.

Keywords: Computational fluid dynamics, Finite difference method, Tandem welding.

Tandem Kaynak İşleminde Sıcaklık Dağılımının Sayısal Analizi

Öz

Bu çalışmada, sabit ve homojen ısı kaynağını içeren ve zamana bağlı olmayan ısı iletimi probleminin, taşınım ısı transferini içeren ve zamana bağlı olmayan ısı iletimi probleminin ayrıca zamana bağlı ısı iletimi probleminin sayısal çözümleri sonlu farklar yöntemi kullanılarak elde edilmiştir. Bu sayısal çözümler analitik çözümlerle doğrulanmıştır. Sayısal çözümler ve analitik çözümler arasındaki uyum gözlemlendikten sonra, tandem kaynak sürecini simüle etmek için bu üç farklı problem birleştirilmiştir. Bu çalışmanın ilk amacı, homojen olmayan hareketli ısı kaynaklarını ve taşınımla ısı transferini içeren bunun yanı sıra zamanın bir fonksiyonu olan ısı iletimi problemi için sayısal bir simülatör sunmaktır. Bu sayısal simülatör, açık ve örtük zaman ayrıklaştırma yöntemlerini içerir. Bu simülatörde; ızgara boyutlarını, zaman adımı boyutlarını, toplam simülasyon süresini, elektrotlar arasındaki mesafeyi, kaynakların gücünün büyüklüğünü, kaynakların hızını değiştirmek mümkündür. İkinci olarak, erimiş havuzun düşük sıcaklık bölgesinde sıvı metalin erken katılaşmasını araştırmak için önerilen sayısal simülatör kullanılarak tek ve çift tel kaynak işlemlerinin sıcaklık dağılımı karşılaştırılmıştır. Son olarak, geliştirilen sayısal simülatör ile ilgili tüm Matlab kodları, diğer araştırmacıların çalışmalarını kolaylaştırmak için makalenin sonuna eklenmiştir.

Anahtar Kelimeler: Hesaplamalı akışkanlar dinamiği, Sonlu farklar yöntemi, Tandem kaynağı.

[1]Sakarya University of Applied Sciences, Department of Mechanical Enginering , Sakarya, Turkey, osman92unal@gmail.com
[2]Sakarya University of Applied Sciences, Department of Mechanical Enginering , Sakarya, Turkey, nuriakkas@subu.edu.tr

[1]https://orcid.org/0000-0003-1101-6561   [2]https://orcid.org/0000-0001-7477-7777

1. Introduction

Tandem welding is well known for its ability to increase welding productivity, as various authors have proved (Chen et al., 2015; Wu et al., 2018; Zhang et al., 2019). Tandem welding technique is employed in the heavy and automotive industries because it has a better productivity and deposition rate than single wire welding (Zargari et al., 2019). Tandem welding has obtained good results in terms of welding speed and deposition rate. Tandem welding can double the rate of deposition in steel welding (Michie, 1999; Goecke et al., 2001) and increase the rate of deposition in aluminum welding by 55% (Lee et al., 2013). When compared to a single wire method, it requires half the welding passes for thick Aluminum plates (Kim et al., 2016). In high speed single-wire welding process, the formation of weld appearance defects is observed due to the premature solidification of liquid metal in low-temperature zone of molten pool (Qin et al., 2021). Twin-wire welding is used to inhibit these defects such as undercut and humping weld (Qin et al., 2015). In this study, the numerical solution of a simplify form of the welding process is developed to compare temperature distribution of single-wire and twin-wire welding. The numerical solutions of single-wire and twin-wire processes may be represented by the transient heat conduction equation that includes non-uniform moving heat source (s) and convective heat transfer term. The analytical solution of this complex problem is not available in literature due to the non-uniform heat sources and convective heat transfer term in transient heat conduction equation. Therefore, the numerical solution is developed to model this sophisticated problem using finite difference method (Smith et al., 1985). The transient heat conduction problem that includes non-uniform moving heat source (s) and convective heat transfer term consists of the steady-state heat conduction problem with uniform heat source, the steady-state heat conduction problem with convective heat transfer and the transient heat conduction problem. These three problems have analytical solution. In this study, once the numerical solutions for the steady-state heat conduction problem with uniform heat source, the steady-state heat conduction problem with convective heat transfer and the transient heat conduction problem were validated with their analytical solutions, these three problems have been combined to obtain numerical model of temperature distribution for single-wire and twin-wire welding processes.

The governing equations for the steady-state heat conduction problem with uniform heat source, the steady-state heat conduction problem with convective heat transfer and the transient heat conduction problem are shown by Equation 1, 2 and 3 (Ozısık, 1993; Grigull and Sandner, 1984), respectively.

$$\frac{d}{dx}\left(k\frac{dT}{dx}\right) + q = 0 \tag{1}$$

$$\frac{d}{dx}\left(k\frac{dT}{dx}\right) - \frac{hP(T-T_\infty)}{A} = 0 \qquad (2)$$

$$\rho c \frac{\partial T}{\partial t} = \frac{\partial}{\partial x}\left(k\frac{\partial T}{\partial x}\right) \qquad (3)$$

The following Equation 4, 5 (Versteeg et al., 2007) and 6 (Ozısık, 1985) indicate the analytical solutions of Equation 1, 2 and 3 in the literature.

$$T = \left[\frac{T_B - T_A}{L} + \frac{q}{2k}(L-x)\right]x + T_A \qquad (4)$$

$$\frac{T-T_\infty}{T_B-T_\infty} = \frac{cosh[n(L-x)]}{cosh(nL)} \qquad (5)$$

$$\frac{T(x,t)}{T_i} = \frac{4}{\pi}\sum_{n=1}^{\infty}\frac{(-1)^{n+1}}{2n-1}exp\left[-\frac{k}{\rho c}\left(\frac{2n\pi-\pi}{2L}\right)^2 t\right] \times cos\left[\left(\frac{2n\pi-\pi}{2L}\right)x\right] \qquad (6)$$

2. Materials and Methods

2.1. Case 1: Steady-State Heat Conduction Problem with Uniform Heat Source

One of the techniques used to obtain the numerical solution of the steady-state heat conduction equation involving uniform heat generation is the finite difference method. The general form of the one dimensional space discretization of Equation 1 using finite difference method is expressed as following Equation 7 (Strikwerda, 2004).

$$k\frac{\frac{T_{i+1}-T_i}{\Delta x} - \frac{T_i - T_{i-1}}{\Delta x}}{\Delta x} + q_i = 0 \qquad (7)$$

It's assumed that, the thermal conductivity (k) in Equation 7 is constant through all nodes. Figure 1 indicates schematic of space discretization and boundary condition for general heat conduction problems.
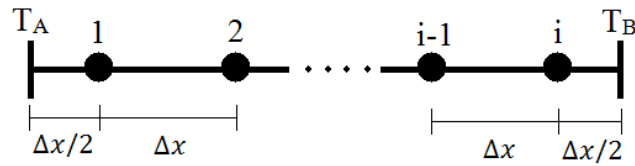
Figure 1. Space Discretization and Boundary Condition.

The discretized equation for node 1 (Equation 8):

$$k\frac{\frac{T_2-T_1}{\Delta x}-\frac{T_1-T_A}{\Delta x/2}}{\Delta x}+q_1=0 \tag{8}$$

The discretized equation for node 2 (Equation 9):

$$k\frac{\frac{T_3-T_2}{\Delta x}-\frac{T_2-T_1}{\Delta x}}{\Delta x}+q_2=0 \tag{9}$$

The discretized equation for node i-1 (Equation 10):

$$k\frac{\frac{T_i-T_{i-1}}{\Delta x}-\frac{T_{i-1}-T_{i-2}}{\Delta x}}{\Delta x}+q_{i-1}=0 \tag{10}$$

The discretized equation for node i (Equation 11):

$$k\frac{\frac{T_B-T_i}{\Delta x/2}-\frac{T_i-T_{i-1}}{\Delta x}}{\Delta x}+q_i=0 \tag{11}$$

There are "i" equations and there are "i" unknowns (T_1, T_2, …, T_{i-1} and T_i). Therefore, this system of equations can be solved (Golub, 1965). Following Equation 12 implies numerical solution of the steady-state heat conduction equation involving uniform heat generation.

$$\begin{bmatrix} -3 & 1 & 0 & \cdots & & 0 & 0 & 0 \\ 1 & -2 & 1 & 0 & & \cdots & 0 & 0 \\ 0 & 1 & -2 & 1 & & 0 & \cdots & 0 \\ & \vdots & & \ddots & & & \vdots & \\ 0 & \cdots & 0 & 1 & -2 & 1 & & 0 \\ 0 & 0 & \cdots & & 0 & 1 & -2 & 1 \\ 0 & 0 & 0 & & \cdots & 0 & 1 & -3 \end{bmatrix} \begin{bmatrix} T_1 \\ T_2 \\ T_3 \\ \vdots \\ T_{i-2} \\ T_{i-1} \\ T_i \end{bmatrix} = \begin{bmatrix} -\frac{q_1\Delta x^2}{k}-2T_A \\ -\frac{q_2\Delta x^2}{k} \\ -\frac{q_3\Delta x^2}{k} \\ \vdots \\ -\frac{q_{i-2}\Delta x^2}{k} \\ -\frac{q_{i-1}\Delta x^2}{k} \\ -\frac{q_i\Delta x^2}{k}-2T_B \end{bmatrix} \tag{12}$$

Figure 2 shows analytical solution and numerical solution for the steady-state heat conduction equation involving uniform heat generation (case 1).
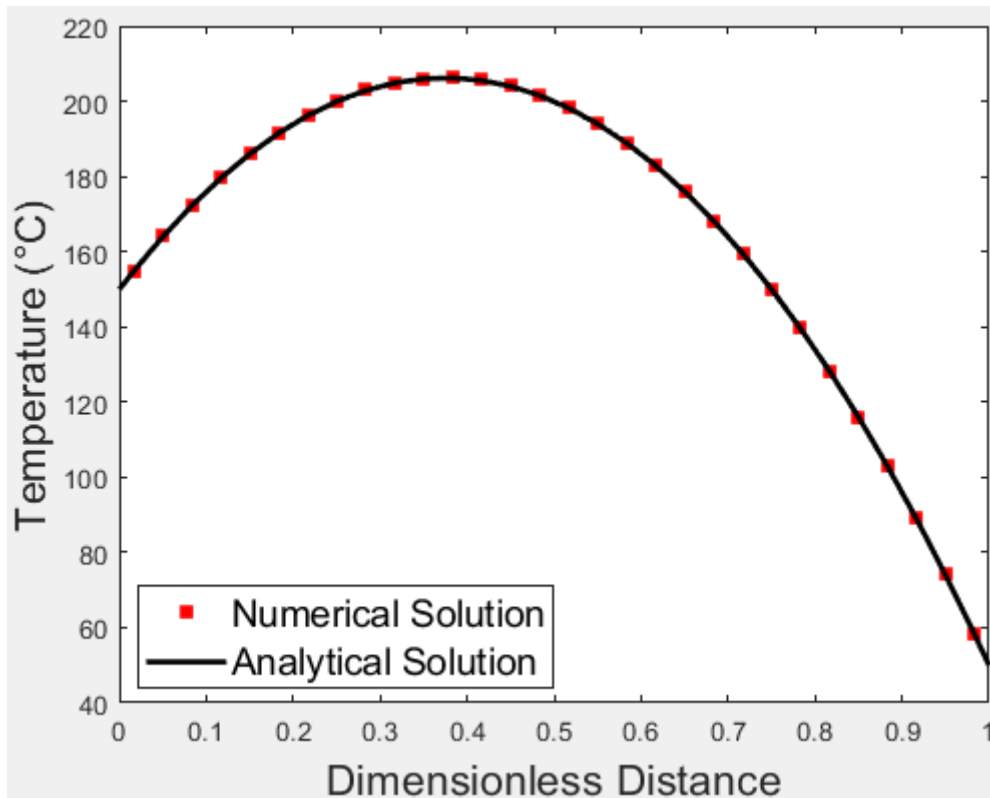
Figure 2. Numerical Solution and Analytical Solution for Case 1.

In Figure 2, it's assumed that left boundary condition (T_A) is 150°C and right boundary condition (T_B) is 50°C. According to Figure 2, there is good agreement between numerical and analytical solutions. The Matlab codes related to case 1 has been added to Appendix A.

2.2. Case 2: Steady-State Heat Conduction Problem with Convective Heat Transfer Term

The general discretized form of Equation 2 is expressed as following Equation 13.

$$k \frac{\frac{T_{i+1}-T_i}{\Delta x}-\frac{T_i-T_{i-1}}{\Delta x}}{\Delta x} - \frac{T_i h P}{A} + \frac{T_\infty h P}{A} = 0 \tag{13}$$

The discretized equation for node 1 (Equation 14):

$$k \frac{\frac{T_2-T_1}{\Delta x}-\frac{T_1-T_A}{\Delta x/2}}{\Delta x} - \frac{T_i h P}{A} + \frac{T_\infty h P}{A} = 0 \tag{14}$$

The discretized equation for node 2 (Equation 15):

$$k \frac{\frac{T_3-T_2}{\Delta x} - \frac{T_2-T_1}{\Delta x}}{\Delta x} - \frac{T_i hP}{A} + \frac{T_\infty hP}{A} = 0 \tag{15}$$

The discretized equation for node i-1 (Equation 16):

$$k \frac{\frac{T_i-T_{i-1}}{\Delta x} - \frac{T_{i-1}-T_{i-2}}{\Delta x}}{\Delta x} - \frac{T_i hP}{A} + \frac{T_\infty hP}{A} = 0 \tag{16}$$

The discretized equation for node i (Equation 17):

$$k \frac{0 - \frac{T_i-T_{i-1}}{\Delta x}}{\Delta x} - \frac{T_i hP}{A} + \frac{T_\infty hP}{A} = 0 \tag{17}$$

Since the number of equations is equal to the number of unknowns, unknown temperature values can be determined. To simplify the solution matrix, a total of four nodes are considered (Equation 18). In the solution system, it's assumed that left boundary condition (T_B) is 250°C, right boundary condition is insulated (the first term is zero in Equation 17 due to the insulation) and ambient temperature is 45°C.

$$\begin{bmatrix} \frac{-3k}{\Delta x^2} - \frac{hP}{A} & \frac{k}{\Delta x^2} & 0 & 0 \\ \frac{k}{\Delta x^2} & \frac{-2k}{\Delta x^2} - \frac{hP}{A} & \frac{k}{\Delta x^2} & 0 \\ 0 & \frac{k}{\Delta x^2} & \frac{-2k}{\Delta x^2} - \frac{hP}{A} & \frac{k}{\Delta x^2} \\ 0 & 0 & \frac{k}{\Delta x^2} & \frac{-2k}{\Delta x^2} - \frac{hP}{A} \end{bmatrix} \times \begin{bmatrix} T_1 \\ T_2 \\ T_3 \\ T_4 \end{bmatrix} = \begin{bmatrix} \frac{-2T_B k}{\Delta x^2} - \frac{hPT_e}{A} \\ -\frac{hPT_e}{A} \\ -\frac{hPT_e}{A} \\ -\frac{hPT_e}{A} \end{bmatrix} \tag{18}$$

In Figure 3, temperature is decreasing due to the convective heat transfer up to the ambient temperature. Figure 3 indicates the validation of the numerical solution with analytical solution. All Matlab codes related to Case 2 have been added to Appendix B.
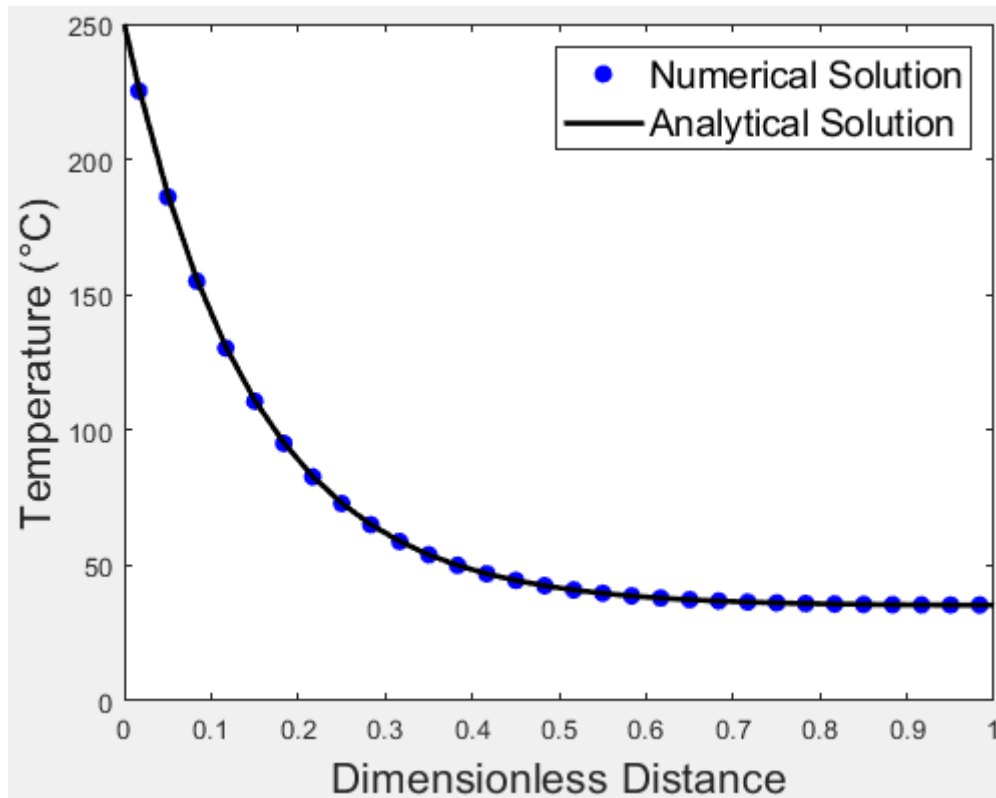
Figure 3. Numerical Solution and Analytical Solution for Case 2.

2.3. Case 3: Transient Heat Conduction Problem

In the numerical solution of transient heat conduction equation, temperature is a function of both space and time. Hence, in addition to space discretization, convenient time discretization technique should be selected to model physical system properly. There are two widely used techniques to discretize time, namely explicit (Rio et al., 2005) and implicit (Lubich and Ostermann, 1995) methods. Although the explicit technique is the simplest method to solve the transient heat conduction problem numerically, it leads to unphysical oscillation at large time step sizes. This technique needs stability requirement to obtain well-posed numerical solution. On the other hand, implicit technique is unconditionally stable (Peaceman, 2000). The full discretized form of Equation 3 using explicit time discretization method and second derivative space discretization technique is shown as following Equation 19.

$$k \frac{\frac{T_{i+1}^{n}-T_{i}^{n}}{\Delta x}-\frac{T_{i}^{n}-T_{i-1}^{n}}{\Delta x}}{\Delta x} = \rho c \frac{T_{i}^{n+1}-T_{i}^{n}}{\Delta t} \qquad (19)$$

The discretized equation for node 1 (Equation 20):

$$k \frac{\frac{T_2^n - T_1^n}{\Delta x} - 0}{\Delta x} = \rho c \frac{T_1^{n+1} - T_1^n}{\Delta t} \qquad (20)$$

In Equation 20, superscript n and n+1 refer to current time step and next time step, respectively. Equation 21 is obtained by rearranging Equation 20 to get the temperature value at the next time step.

$$T_1^{n+1} = T_1^n + \frac{k\Delta t}{\rho c} \frac{\frac{T_2^n - T_1^n}{\Delta x} - 0}{\Delta x} \qquad (21)$$

The discretized equation for node 2 (Equation 22 and 23):

$$k \frac{\frac{T_3^n - T_2^n}{\Delta x} - \frac{T_2^n - T_1^n}{\Delta x}}{\Delta x} = \rho c \frac{T_2^{n+1} - T_2^n}{\Delta t} \qquad (22)$$

$$T_2^{n+1} = T_2^n + \frac{k\Delta t}{\rho c} \frac{\frac{T_3^n - T_2^n}{\Delta x} - \frac{T_2^n - T_1^n}{\Delta x}}{\Delta x} \qquad (23)$$

The discretized equation for node i-1 (Equation 24 and 25):

$$k \frac{\frac{T_i^n - T_{i-1}^n}{\Delta x} - \frac{T_{i-1}^n - T_{i-2}^n}{\Delta x}}{\Delta x} = \rho c \frac{T_{i-1}^{n+1} - T_{i-1}^n}{\Delta t} \qquad (24)$$

$$T_{i-1}^{n+1} = T_{i-1}^n + \frac{k\Delta t}{\rho c} \frac{\frac{T_i^n - T_{i-1}^n}{\Delta x} - \frac{T_{i-1}^n - T_{i-2}^n}{\Delta x}}{\Delta x} \qquad (25)$$

The discretized equation for node i (Equation 26 and 27):

$$k \frac{\frac{T_B^n - T_i^n}{\Delta x/2} - \frac{T_i^n - T_{i-1}^n}{\Delta x}}{\Delta x} = \rho c \frac{T_i^{n+1} - T_i^n}{\Delta t} \qquad (26)$$

$$T_i^{n+1} = T_i^n + \frac{k\Delta t}{\rho c} \frac{\frac{T_B^n - T_i^n}{\Delta x/2} - \frac{T_i^n - T_{i-1}^n}{\Delta x}}{\Delta x} \qquad (27)$$

This explicit time discretization technique is a time march method. The next time step values are calculated using current time step values. Thus, the coefficient of interested temperature at

current time step (for example the total coefficient of T_i^n in Equation 27) must be positive in order to obtain stable numerical solution for explicit time discretization method. The stability requirement for explicit scheme:

$$T_i^{n+1} = T_i^n \left(1 - \frac{2k\Delta t}{\rho c \Delta x^2}\right) + \frac{k\Delta t}{\rho c} \frac{\frac{T_{i+1}^n}{\Delta x} - \frac{-T_{i-1}^n}{\Delta x}}{\Delta x} \tag{28}$$

The coefficient of T_1^n in Equation 28 must be positive to provide stability requirement for explicit time discretization method.

$$\left(1 - \frac{2k\Delta t}{\rho c \Delta x^2}\right) > 0 \tag{29}$$

Equation 30 is obtained by rearranging Equation 29.

$$\Delta t < \frac{\rho c \Delta x^2}{2k} \tag{30}$$

The Equation 30 implies that time step sizes must be lesser than $\rho c \Delta x^2 / 2k = 0.22$ to get stable numerical solution.
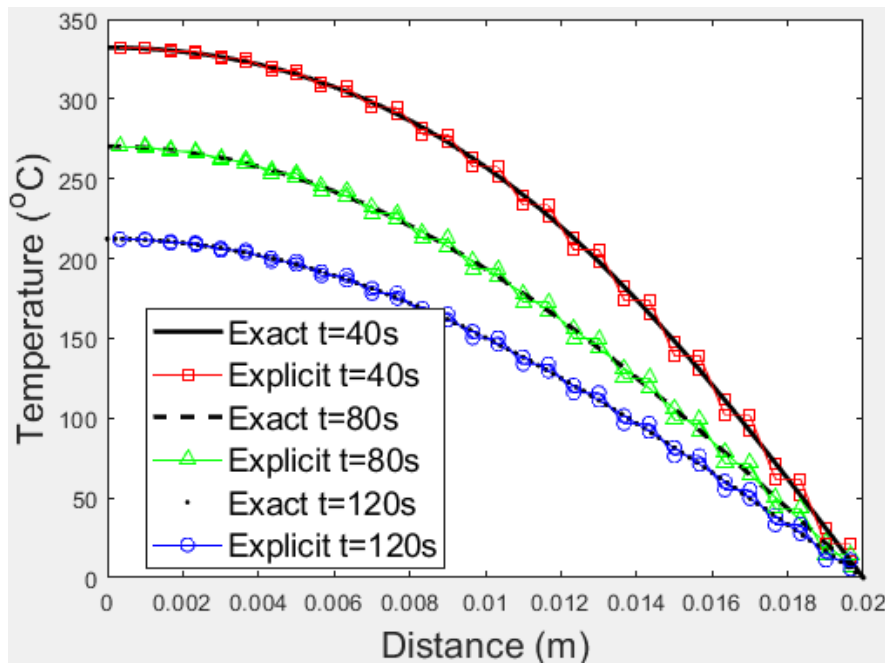
Figure 4. Numerical Solution and Analytical Solution for Case 3 (dt=0.2222 seconds).

The time step size is greater than 0.22 in Figure 4 (0.2222>0.22). Hence, there are some undesired and unphysical oscillations (Torabi et al., 2014) in Figure 4. These numerical results are not stable and reliable. On the other hand, Figure 5 indicates sensible and stable numerical results due to the using small time step size (0.2<0.22). There are good agreements between numerical and analytical solutions in Figure 5. It's important note that all Matlab codes related to Case 3 have been added to Appendix C.
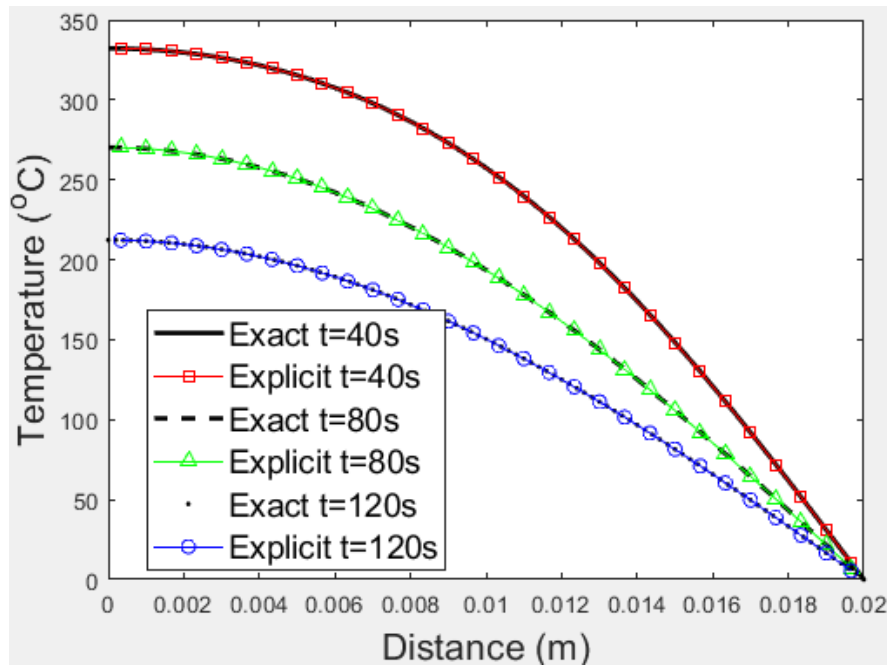
Figure 5. Numerical Solution and Analytical Solution for Case 3 (dt=0.2 seconds).

2.4. Case 4: Transient Heat Conduction Problem with Non-uniform Moving Heat Source (s) and Convective Heat Transfer Term

After validation of numerical solution of Case 1, Case 2 and Case 3 with their analytical solutions, these three cases were combined to model simplify form of tandem welding process. The following Equation 31 indicates governing equation of the transient heat conduction problem with non-uniform moving heat source (s) and convective heat transfer term.

$$\rho c \frac{\partial T}{\partial t} = \frac{\partial}{\partial x}\left(k \frac{\partial T}{\partial x}\right) + q - \frac{hP(T - T_\infty)}{A} \tag{31}$$

The Equation 32 shows numerical solution of Equation 31 using implicit time discretization and second derivative space discretization technique for node 1.

$$\rho c \frac{T_1^{n+1}-T_1^n}{\Delta t} = k \frac{\frac{T_2^{n+1}-T_1^{n+1}}{\Delta x} - \frac{T_1^{n+1}-T_A^{n+1}}{\Delta x/2}}{\Delta x} + q_1^{n+1} - \frac{hP(T_1^{n+1}-T_\infty)}{A} \tag{32}$$

The discretized equation for interior nodes (Equation 33):

$$\rho c \frac{T_i^{n+1}-T_i^n}{\Delta t} = k \frac{\frac{T_{i+1}^{n+1}-T_i^{n+1}}{\Delta x} - \frac{T_i^{n+1}-T_{i-1}^{n+1}}{\Delta x}}{\Delta x} + q_i^{n+1} - \frac{hP(T_i^{n+1}-T_\infty)}{A} \tag{33}$$

The discretized equation for last node (Equation 34):

$$\rho c \frac{T_i^{n+1}-T_i^n}{\Delta t} = k \frac{\frac{T_B^{n+1}-T_i^{n+1}}{\Delta x/2} - \frac{T_i^{n+1}-T_{i-1}^{n+1}}{\Delta x}}{\Delta x} + q_i^{n+1} - \frac{hP(T_i^{n+1}-T_\infty)}{A} \tag{34}$$

The matrix solution should be calculated for each time steps to get implicit numerical solution of Equation 31. It's assumed that there are three nodes to simplify solution matrix (Equation 35).

$$\begin{bmatrix} \frac{-3k}{\Delta x^2}-\frac{\rho c}{\Delta t}-\frac{hP}{A} & \frac{k}{\Delta x^2} & 0 \\ \frac{k}{\Delta x^2} & \frac{-2k}{\Delta x^2}-\frac{\rho c}{\Delta t}-\frac{hP}{A} & \frac{k}{\Delta x^2} \\ 0 & \frac{k}{\Delta x^2} & \frac{-3k}{\Delta x^2}-\frac{\rho c}{\Delta t}-\frac{hP}{A} \end{bmatrix} \times \begin{bmatrix} T_1 \\ T_2 \\ T_3 \end{bmatrix} = \begin{bmatrix} \frac{-\rho c T_i^n}{\Delta t}-q_i^{n+1}-\frac{2kT_A}{\Delta x^2}-\frac{hPT_e}{A} \\ \frac{-\rho c T_i^n}{\Delta t}-q_i^{n+1}-\frac{hPT_e}{A} \\ \frac{-\rho c T_i^n}{\Delta t}-q_i^{n+1}-\frac{2kT_A}{\Delta x^2}-\frac{hPT_e}{A} \end{bmatrix} \tag{35}$$

2.5. Experimental Study

One of the most common arc welding techniques is single wire welding. Because of the higher current, a smaller diameter wire increases deposition rate at same current. Higher currents and thus higher deposition rates are involved in the current range for a bigger size. A smaller wire diameter results in a more deeply penetrating as well as relatively narrow weld bead. The advantages of tandem welding over single wire welding process are high welding speed, high performance, and the filling large weld gaps between two work pieces (Tušek et al., 2005). Figure 6 shows schematic views of the single wire welding and tandem welding processes.
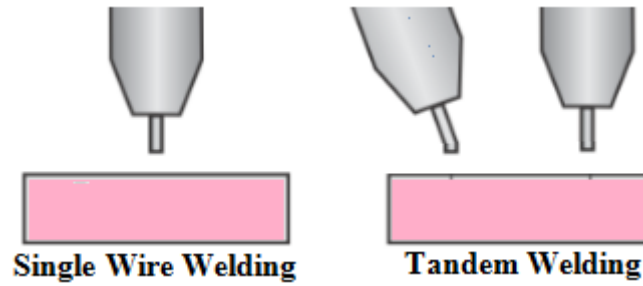
Figure 6. Schematic views of the single wire and tandem welding processes.

Tandem welding is a technique that uses two separate welding systems which are synchronized. Separate wire feeders with a gas nozzle and isolated contact tips feed the unconnected wire electrodes into a torch hose pack. The weld pool is created by two arcs. A Twin Controller can be used to synchronize both wire electrodes. A wire electrode can also be connected and disconnected. It is possible to weld in both directions. As a result, there is a great deal of mobility. This method is far more stable, allowing for extremely high welding speeds on thin sheets. This technique has a high deposition rate for thick sheets, allowing for a much larger weld seam volume.

All experiments in this study were carried out in Turkish Railway Vehicles Industry Incorporated (TURASAS). Welding experiment was conducted on the Aluminum alloy sheet with dimensions of 600 mm × 80 mm × 3 mm. The material used in this study is Al6005 alloy. Mechanical properties of Al6005 alloy used in this study are Density: 2.70 g/cm^3, Young's modulus: 68 GPa, Ultimate tensile strength: 300 MPa, Yield strength: 250 MPa, Thermal expansion: 23 μm/m-K. The chemical composition of Al6005 alloy is 0.40 % Si, 0.175 %, 0.05 % Cu, 0.05 % Mn, 0.675 % Mg, 0.05 % Cr, 0.05 % Zn, 0.05 % Ti and 98.5 % Al (Bajor et al., 2021). 5356 AlMg5 type electrodes were used in single wire and tandem welding processes in this study. The welding wire feed rate is 10.4 m/min, weld current is 186 A and weld voltage is 21.8 V. Figure 7 shows tandem welding processes in TURASAS.

Figure 7. Tandem welding processes in TURASAS.

3. Findings and Discussion

The numerical simulator of the transient heat conduction problem with non-uniform moving heat source (s) and convective heat transfer term has been improved for different number of nodes, desired time step sizes, single and twin-wire welding processes (see Appendix D). The Figure 8 shows the numerical result of Equation 31 using 200 nodes instead of using 3 nodes.
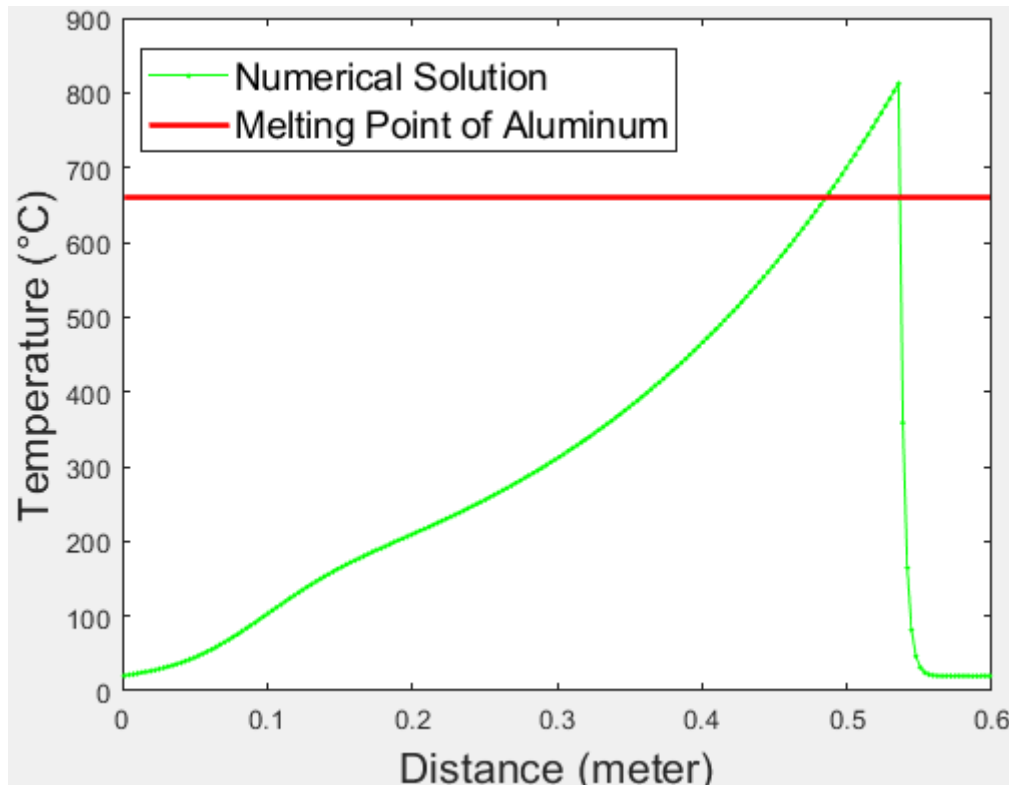
Figure 8. Single-Wire Welding Process.

In Figure 8, it's been assumed that there is a single moving heat source, the ambient temperature is 20°C, the left and right boundary conditions are 20°C. According to Figure 8, the temperature decreases rapidly below to melting point of aluminum after welding and it causes weld appearance defects due to the premature solidification of liquid metal. The Figure 9 indicates the numerical solution for transient heat conduction problem with non-uniform moving heat sources and convective heat transfer term. It may represent a simple form of tandem welding process.
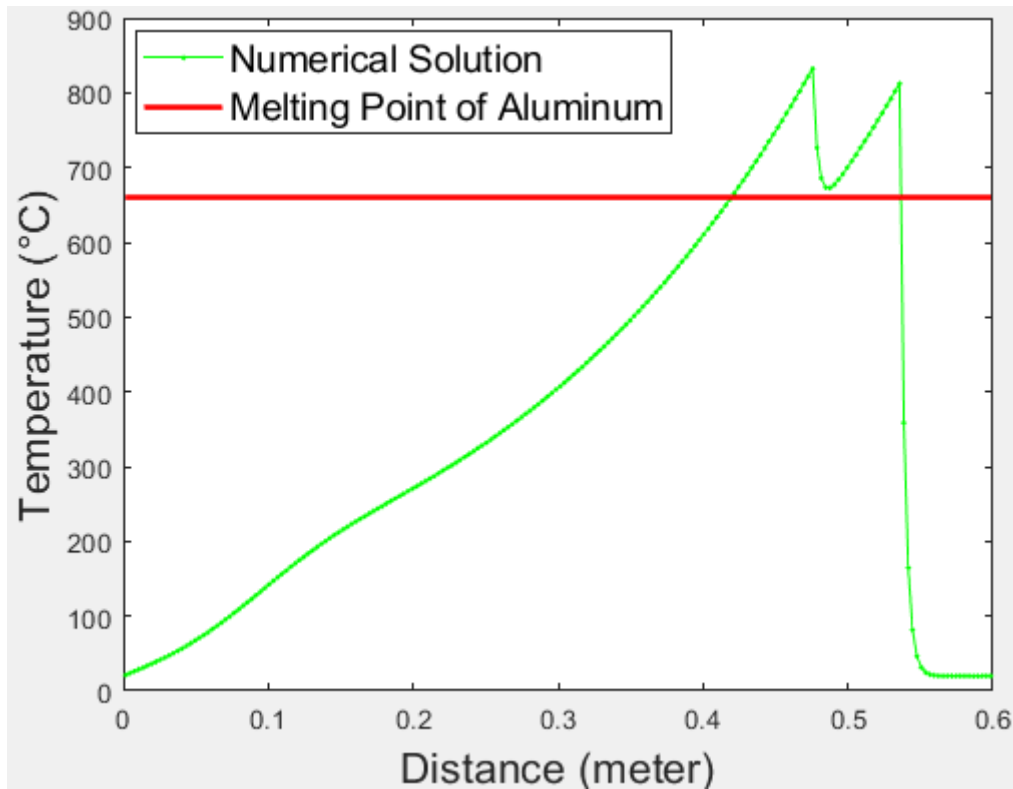
Figure 9. Numerical Solution for Transient Heat Conduction Problem with Non-uniform Moving Heat Source (s) and Convective Heat Transfer Term (Tandem Welding Process).

In Figure 9, there are two electrodes with different power. The weld appearance defects such as porosity, poor penetration, undercut, and etc. may be prevented using tandem welding process. The total time for solidification of liquid metal at low-temperature zone is extended using the second electrode and weld appearance defects may be inhibited.

Figure 10 shows temperature distribution of aluminum welding process. It was obtained using Fluke Thermal Imager. Figure 10 includes three experimental results. Experimental errors were minimized using these three experimental results. The maximum temperature was used to validate numerical results with experimental study. The maximum temperature of numerical result is 832.527 °C. The maximum temperatures of experimental results are 833.3 °C, 826.3 °C and 831.8 °C. The average temperature of experimental results is 830.467 °C. The numerical result is very close to the experimental result. These obtained data clearly show that the results of the numerical method are validated with the results obtained from the experimental study.
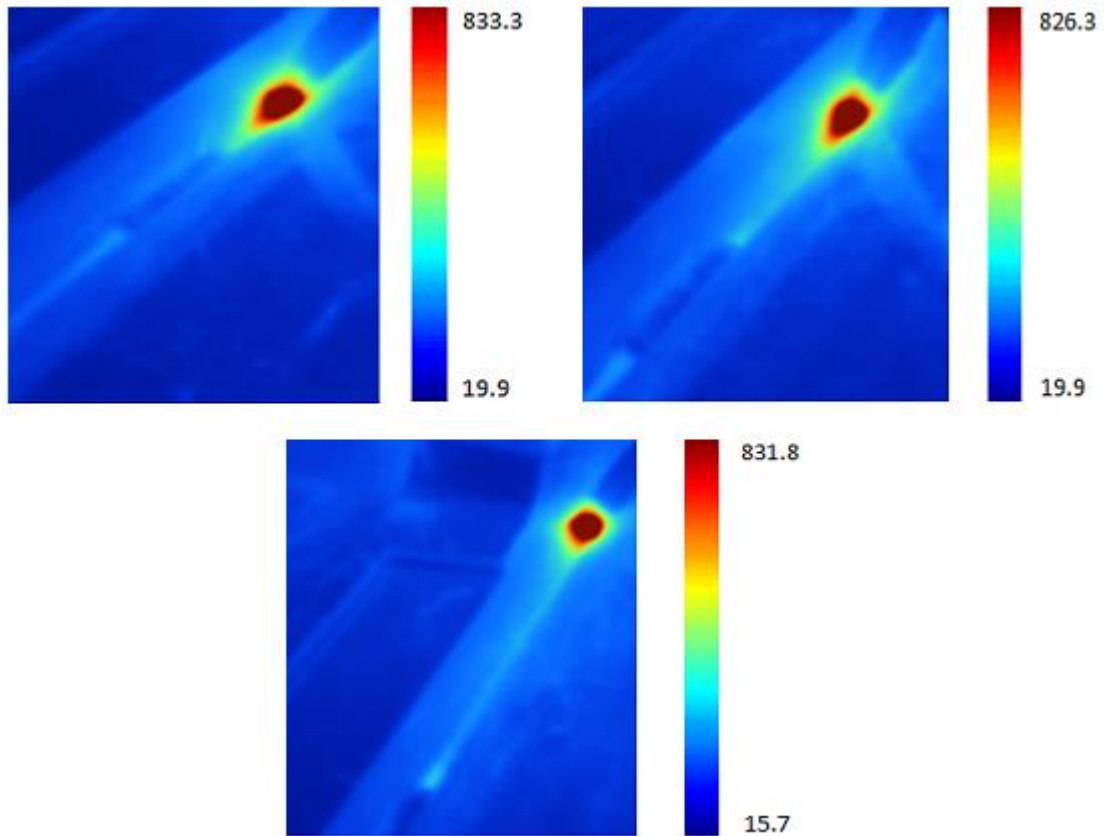
Figure 10. Temperature distributions of aluminum welding process (°C).

4. Conclusions and Recommendations

Firstly, the numerical solutions of three different cases related to heat conduction problem have been modeled and validated with their analytical solutions. Secondly, these three different cases namely the steady-state heat conduction problem with uniform heat source, the steady-state heat conduction problem with convective heat transfer and the transient heat conduction problem have been merged to model numerical solution of transient heat conduction problem with non-uniform moving heat source (s) and convective heat transfer term. Thirdly, the single and twin-wire welding processes have been compared to investigate the temperature distribution of low-temperature zone of molten pool. It's been observed that rapid decreasing of temperature at low-temperature zone can be prevented and controlled using second electrode. Fourthly, the temperature distributions of the aluminum welding process were obtained using the Fluke Thermal Imager. Three thermal images were taken to minimize experimental errors. The maximum temperature was taken into consideration to validate numerical results with experimental study. The maximum temperature of numerical result was obtained as 832.527 °C using numerical simulation. The average temperature of three experimental results was obtained as 830.467 °C. It is calculated that the numerical result is very close to the experimental result with 0.248 % error. It clearly shows that

the results of the numerical method are validated with the results obtained from the experimental study. Finally, all Matlab codes related to numerical and analytical simulations have been added to Appendix.

Acknowledgements

Authors' Contributions

All authors contributed equally to the study.

Statement of Conflicts of Interest

There is no conflict of interest between the authors.

Statement of Research and Publication Ethics

The author declares that this study complies with Research and Publication Ethics.

References

Bajor, T., Kwapisz, M., Krakowiak, M., & Jurczak, H. (2021). THE ANALYSIS OF THE EXTRUSION PROCESS OF Al 6005 ALLOY SECTION. Journal of Chemical Technology and Metallurgy, 56(3), 637-642.

Chen, D., Chen, M., & Wu, C. (2015). Effects of phase difference on the behavior of arc and weld pool in tandem P-GMAW. Journal of Materials Processing Technology, 225, 45-55.

Goecke, S., Berlin, F. U. B. T., Hedegård, J., Joining, S. I. M. R., & AB, E. W. E. (2001). Tandem Mig/Mag Welding. A Welding Review Published by Esab, 56(2-3), 24-28.

Golub, G. (1965). Numerical methods for solving linear least squares problems. Numerische Mathematik, 7(3), 206-216.

Grigull, U., & Sandner, H. (1984). Heat conduction.

Kim, C., Ahn, Y., Lee, K. B., & Kim, D. (2016). High-deposition-rate position welding of Al 5083 alloy for spherical-type liquefied natural gas tank. Proceedings of the Institution of Mechanical Engineers, Part B: Journal of Engineering Manufacture, 230(5), 818-824.

Lee, K. B., Kim, C., & Kim, D. S. (2013). High deposition rate pulse gas metal arc welding for Al 5083 thick plate. Proceedings of the Institution of Mechanical Engineers, Part B: Journal of Engineering Manufacture, 227(6), 848-854.

Lubich, C., & Ostermann, A. (1995). Linearly implicit time discretization of non-linear parabolic equations. IMA journal of numerical analysis, 15(4), 555-583.

Michie, K. (1999). Twin-wire GMAW: process, characteristics and applications. Welding Journal, 78(5), 31-34.

Özışık, M. N. (1993). Heat conduction. John Wiley & Sons.

Ozisik, M. N. (1985). Heat transfer: a basic approach (Vol. 1). New York: McGraw-Hill.

Peaceman, D. W. (2000). Fundamentals of numerical reservoir simulation. Elsevier.

Qin, G., Feng, C., & Ma, H. (2021). Suppression mechanism of weld appearance defects in tandem TIG welding by numerical modeling. Journal of Materials Research and Technology.

Qin, G., Meng, X., & Fu, B. (2015). High speed tandem gas tungsten arc welding process of thin stainless steel plate. Journal of Materials Processing Technology, 220, 58-64.

Rio, G., Soive, A., & Grolleau, V. (2005). Comparative study of numerical explicit time integration algorithms. Advances in Engineering Software, 36(4), 252-265.

Smith, G. D., Smith, G. D., & Smith, G. D. S. (1985). Numerical solution of partial differential equations: finite difference methods. Oxford university press.

Strikwerda, J. C. (2004). Finite difference schemes and partial differential equations. Society for Industrial and Applied Mathematics.

Torabi Ziaratgahi, S., Marsh, M. E., Sundnes, J., & Spiteri, R. J. (2014). Stable time integration suppresses unphysical oscillations in the bidomain model. Frontiers in Physics, 2, 40.

Tušek, J., Umek, I., & Bajcer, B. (2005). Weld-cost saving accomplished by replacing single-wire submerged arc welding with triple-wire welding. Science and Technology of Welding and Joining, 10(1), 15-22.

Versteeg, H. K., & Malalasekera, W. (2007). An introduction to computational fluid dynamics: the finite volume method. Pearson education.

Wu, K., Ding, N., Yin, T., Zeng, M., & Liang, Z. (2018). Effects of single and double pulses on microstructure and mechanical properties of weld joints during high-power double-wire GMAW. Journal of Manufacturing Processes, 35, 728-734.

Zargari, H. H., Ito, K., Kumar, M., & Sharma, A. (2020). Visualizing the vibration effect on the tandem-pulsed gas metal arc welding in the presence of surface tension active elements. International Journal of Heat and Mass Transfer, 161, 120310.

Zhang, L., Su, S., Wang, J., & Chen, S. J. (2019). Investigation of arc behaviour and metal transfer in cross arc welding. Journal of Manufacturing Processes, 37, 124-129.

Symbols

c = *specific heat capacity*

h = *convective heat transfer coefficient*

k = *thermal conductivity*

P = *perimeter*

q = *heat source*

T = *temperature*

ρ = *density*

Δt = *timestep*

Δx = *space interval*

Subscripts

i = *index for nodes in the x direction*

$i-1$ = *previous node*

$i+1$ = *next node*

Superscripts

n = *old timestep*

$n+1$ = *current timestep*

Appendices

Appendix A. Case 1: Steady-State Heat Conduction Problem with Uniform Heat Source.

```
tic; clc; clearvars;
L=0.02;%Length
I=30;%Number of nodes at i-direction
dx=L/I;%Space interval
X=[0 dx/2:dx:L-dx/2 L]';%Distance
k=0.5;%Thermal conductivity: W/(m.°C) = W/(m.K)
TA=150; TB=50;%Boundary Condition(°C)
q=zeros(I,1);
q(1:I,1)=10^6;%Heat generation(W/m3)
A=zeros(I,I); B=zeros(I,1);
%%Numerical Solution
for i=1:I
if i==1
A(i,i)=-3; A(i,i+1)=1;
B(i,1)=-q(i,1)*dx^2/k-2*TA;
elseif 1<i && i<I
A(i,i-1)=1; A(i,i)=-2; A(i,i+1)=1;
B(i,1)=-q(i,1)*dx^2/k;
elseif i==I
A(i,i-1)=1; A(i,i)=-3;
B(i,1)=-q(i,1)*dx^2/k-2*TB;
end
end
Tn=sparse(A)\sparse(B);
%set(gcf, 'Units', 'Normalized', 'OuterPosition', [0 0 1 1]);
plot((dx/2:dx:L-dx/2)/I/dx,Tn,'rs','markerfacecolor','r');
xlabel('Dimensionless Distance','fontsize',16)
ylabel('Temperature (°C)','fontsize',16)
%%Analytical Solution
if gradient(q)==0
q=q(1);
Ta=((TB-TA)/L+q/2/k*(L-X)).*X+TA;
hold on
plot(X/I/dx,Ta,'k-','linewidth',2);
legend('Numerical Solution','Analytical Solution')
end
toc
```

Appendix B. Case 2: Steady-State Heat Conduction Problem with Convective Heat Transfer Term.

```
tic; clc; clearvars;
L=0.02;%Length
I=30;%Number of nodes at i-direction
dx=L/I; dy=dx;%Space interval
X=[0 dx/2:dx:L-dx/2 L]';%Distance
k=0.5;%Thermal conductivity: W/(m.°C) = W/(m.K)
h=10;%Convective heat transfer coefficient: W/(m2.K) = W/(m2.°C)
H=h*2*(dx+dy)/dx/dy;
```

```
Te=35;%Ambient(environment) temperature(°C)
TB=250;%Boundary Condition(°C)
A=zeros(I,I); B=zeros(I,1);
%%Numerical Solution
for i=1:I
if i==1
A(i,i)=-3*k/dx^2-H; A(i,i+1)=k/dx^2;
B(i,1)=-2*TB*k/dx^2-H*Te;
elseif 1<i && i<I
A(i,i-1)=k/dx^2; A(i,i)=-2*k/dx^2-H; A(i,i+1)=k/dx^2;
B(i,1)=-H*Te;
elseif i==I
A(i,i-1)=k/dx^2; A(i,i)=-k/dx^2-H;
B(i,1)=-H*Te;
end
end
Tn=sparse(A)\sparse(B);
%set(gcf, 'Units', 'Normalized', 'OuterPosition', [0 0 1 1]);
plot((dx/2:dx:L-dx/2)/I/dx,Tn,'bo','markerfacecolor','b');
xlabel('Dimensionless Distance','fontsize',16)
ylabel('Temperature (°C)','fontsize',16)
%%Analytical Solution
n=sqrt(h*2*(dx+dy)/k/dx/dy);
Ta=Te+(TB-Te)*cosh(n*(L-X))./cosh(n*L);
hold on
plot(X/I/dx,Ta,'k-','linewidth',2);
legend('Numerical Solution','Analytical Solution')
toc
```

Appendix C. Case 3: Transient Heat Conduction Problem.

```
tic; clc; clearvars;
L=0.02;%m (2cm)
k=10;%W/(m.K)
rc=1e7;%J/(m3K)
N=30;%Number of space nodes
t0=0;%second, initial time
tf=120;%second, final time
dt=2/9;%Time step interval
%Note:To get 3 different graphics, tf/dt should be divided into three.
T0=350;%Initial Condition, oC
T_L=0;%Boundary Condition, oC
tr=tf/dt+1;%Time resolution of analytical solution
sr=101;%Space resolution of analytical solution
sumr=100;%Sum resolution of analytical solution
dx=L/N;%Space interval
x=dx/2:dx:L-dx/2;%Node location
n=(tf-t0)/dt+1;%Number of time steps
T=zeros(N,n);
T(:,1)=T0;%K (200oC):Initial Condition
%Stability condition of explicit method:
fprintf('Stability condition: dt<%.2f \n',rc*dx^2/(2*k));
for t=1:n-1 %time loop
for i=1:N %space loop
if i==1
T(i,t+1)=T(i,t)+k*dt/(rc*dx^2)*(T(i+1,t)-T(i,t));
elseif 1<i && i<N
T(i,t+1)=T(i,t)+k*dt/(rc*dx^2)*(T(i+1,t)-2*T(i,t)+T(i-1,t));
elseif i==N
T(i,t+1)=T(i,t)+k*dt/(rc*dx^2)*(2*T_L-3*T(i,t)+T(i-1,t));
end
end
end
```

```matlab
%Analytical Solution: Özisik (1985)
T_a=zeros(sr,tr);
o=1;
for t_a=linspace(t0,tf,tr)
p=1;
for x_a=linspace(0,L,sr)
sum=0;
for m=1:sumr
sum=sum+(-1)^(m+1)/(2*m-1)*exp(-k/rc*((2*m-1)*pi/(2*L))^2*t_a)*cos(((2*m-
1)*pi/(2*L))*x_a);
end
T_a(p,o)=T0*4/pi*sum;
p=p+1;
end
o=o+1;
end
t_a=linspace(t0,tf,tr);
x_a=linspace(0,L,sr);
plot(x_a,T_a(:,(tf/3)/dt+1),'k-','linewidth',2)
hold on
plot(x,T(:,(tf/3)/dt+1),'rs-')
plot(x_a,T_a(:,(tf*2/3)/dt+1),'k--','linewidth',2)
plot(x,T(:,(tf*2/3)/dt+1),'g^-')
plot(x_a,T_a(:,end),'k.','linewidth',2)
plot(x,T(:,end),'bo-')
xlabel('Distance (m)','fontsize',16)
ylabel('Temperature (^oC)','fontsize',16)
title(sprintf('T_L=%d^oC  Mesh=%d dt=%.2fs
SC:dt<%.2f',T_L,N,dt,rc*dx^2/(2*k)),'fontsize',16)
legend({sprintf('Exact t=%ds',tf/3),sprintf('Explicit
t=%ds',tf/3),sprintf('Exact t=%ds',tf*2/3),sprintf('Explicit
t=%ds',tf*2/3),sprintf('Exact t=%ds',tf),sprintf('Explicit
t=%ds',tf)},'FontSize',14,'Location', 'Best')
```

Appendix D. Transient Heat Conduction Problem with Non-uniform Moving Heat Source (s)

and Convective Heat Transfer Term.

```matlab
tic; clc; clearvars;
tt=15;%Total simulation time(second)
dt=0.1;%Time interval(second)
thickness=0.003;%(meter)
dr=0.027;%Row interval(meter)
cn=200;%Column number
dc=0.003;%Column interval(meter)
C=dc/2:dc:cn*dc-dc/2;%Column distance
k=167;%Thermal conductivity: W/(m.°C) = W/(m.K)
rc=2.7*10^6*0.9; %g/m3 * J/(g.K) = J/(m3.K)
h=425;%Convective heat transfer coefficient: W/(m2.K) = W/(m2.°C)
H=h*2*(dc+dr)/dc/dr;
Te=20;%Ambient(environment) temperature(°C)
Tp(1:cn,1)=20;%Initial Condition(°C)
TA=20; TB=20;%Boundary Condition(°C)
VI1=21*230;%Volt*Amper
E1=VI1/thickness/dr/dc;%Heat generation(W/m3)
VI2=11*110;%Volt*Amper
E2=VI2/thickness/dr/dc;%Heat generation(W/m3)
Q=1;%Explicit(Q=0) & Implicit(Q=1)
%%Numerical Solution
Tn(1:cn)=NaN;
A=zeros(cn,cn); B=zeros(cn,1);
for t=1:tt/dt%Time iteration
q=zeros(cn,1);
```

```
q(cn/20-1+t,1)=E2; q(cn/20+20-1+t,1)=E1;
for i=1:cn
if i==1 && Q==0
Tn(i)=Tp(i)+dt/rc*(k/dc^2*(2*TA-3*Tp(i)+Tp(i+1))+q(i,1)-H*(Tp(i)-Te));
elseif i==1 && Q==1
A(i,i)=-3*k/dc^2-rc/dt-H; A(i,i+1)=k/dc^2;
B(i,1)=-rc*Tp(i)/dt-q(i,1)-k*2*TA/dc^2-H*Te;
elseif 1<i && i<cn && Q==0
Tn(i)=Tp(i)+dt/rc*(k/dc^2*(Tp(i-1)-2*Tp(i)+Tp(i+1))+q(i,1)-H*(Tp(i)-Te));
elseif 1<i && i<cn && Q==1
A(i,i-1)=k/dc^2; A(i,i)=-2*k/dc^2-rc/dt-H; A(i,i+1)=k/dc^2;
B(i,1)=-rc*Tp(i)/dt-q(i,1)-H*Te;
elseif i==cn && Q==0
Tn(i)=Tp(i)+dt/rc*(k/dc^2*(Tp(i-1)-3*Tp(i)+2*TB)+q(i,1)-H*(Tp(i)-Te));
elseif i==cn && Q==1
A(i,i-1)=k/dc^2; A(i,i)=-3*k/dc^2-rc/dt-H;
B(i,1)=-rc*Tp(i)/dt-q(i,1)-k*2*TB/dc^2-H*Te;
end
end
if Q==1; Tn=sparse(A)\sparse(B); end
Tp=Tn;
%set(gcf, 'Units', 'Normalized', 'OuterPosition', [0 0 1 1]);
plot(dc/2:dc:cn*dc-dc/2,Tn,'go-','markerfacecolor','g','markersize',1.5);
hold on
plot([dc/2 cn*dc-dc/2],[660.3 660.3],'r-','linewidth',2);
xlabel('Distance (meter)','fontsize',16)
ylabel('Temperature (°C)','fontsize',16)
legend('Numerical Solution','Melting Point of Aluminum')
title(sprintf('1D Sim: time=%1.1f second',t*dt),'fontsize',16)
hold off
pause(0.001)
end
toc
```